VIRTUAL INERTIA CONTROL OF DFIG-BASED WIND TURBINES FOR DYNAMIC GRID FREQUENCY SUPPORT

Xiaorong Zhu[1], Yi Wang[1], Lie Xu[2], Xiangyu Zhang[1], Heming Li[1]

[1]*School of Electrical and Electronic Engineering, North China Electric Power University, Baoding 071003, China*
[2] *School of Electronics, Electrical Engineering and Computer Science, Queen's University of Belfast, Belfast BT9 5AH, UK*
E-mail: yi.wang@ncepubd.edu.cn

Abstract

This paper investigates virtual inertia control of doubly fed induction generator (DFIG)-based wind turbines to provide dynamic frequency support in the event of abrupt power change. The model and control scheme of the DFIG is analysed. The relationships among the virtual inertia, the rotor speed and the network frequency variation are then investigated. The "hidden" kinetic energy that can be released to contribute to the grid inertia by means of shifting the operating point from the maximum power tracking curve to a virtual inertia control curve is investigated. The virtual inertia control strategy based on shifting power tracking curves of the DFIG is proposed and the calculation method for determining these virtual inertia control curves is presented. A three-machine system with 20 percent of wind penetration is used to validate the proposed control strategy. Simulation results show that by the proposed control strategy, DFIG based wind farms have the capability of providing dynamic frequency support to frequency deviation, and thus improving the dynamic frequency performance of the grid with high wind power penetration.

1 Introduction

Wind power generation is developing fast globally. However, the increasing penetration of wind generation in power system has brought up new technical challenges, such as frequency control, system protection, balance control, transient stability and voltage stability. Among these technical issues, the system inertia plays an extremely important role as it determines the sensitivity of system frequency to supply demand imbalances. During a frequency event, the dynamic grid frequency response is initially supported by the system inertia.

DFIG-based wind turbines have become the preferred option for large scale wind farms due to their ability to provide the benefits of variable-speed operation cost-effectively. However, operating a large number of DFIG-based wind turbines in place of conventional plants will reduce the effective inertia of the system. This is due to the fact that the DFIG control system decouples the mechanical and electrical systems and thus it prevents the generator from responding to system frequency changes.

Similar to conventional generators, wind turbines have a significant amount of kinetic energy stored in the rotating mass of their blades. In case of variable-speed wind turbines, this energy will not naturally contribute to the inertia of the grid. Therefore, additional control is needed to make the "hidden inertia" available to the grid. In [1] the factors affecting inertial response of a variable-speed wind energy conversion system (WECS) are studied. In [2-3] some techniques to emulate additional inertia using WECS are presented. The frequency support is a combination of inertial control, using the kinetic energy stored in the rotating masses, and a proportional control of frequency deviation. Once the transient contribution of the wind generator finishes, its rotor speed differs from the optimal value. In [4] an additional control action is added to recover the rotor speed to the optimal value. However, an oscillation of the injected power is clearly observed. An algorithm to extract the maximum kinetic energy without stall the turbine is proposed in [5], in which the electrical torque is increased step-wise by 20% at the time of the disturbances and is ramped down considering the governor time constant. However, controlling power or torque requires different strategies. In [6], an inertia control scheme of DFIG to extract energy from the turbine in a stable way is proposed, however the strategy is not investigated in detail and the rotor speed can not recover to its optimal value after the dynamic frequency support.

In this paper, a novel inertial control of DFIG-based wind turbines is investigated. In the event of dynamic frequency changes, by shifting the operating point from the maximum power tracking curve to the virtual inertial control curve, a step electrical power reference of the rotor side converter (RSC) is generated and the kinetic energy is released / increased to contribute to grid inertia. The rotor speed recovery strategy is proposed to recover it to the optimal value when the system frequency returns to a safe margin. Simulation studies based on a power network with 20% installed wind generation capacity are performed to demonstrate the benefits of the proposed schemes.

2 Modelling and control of DFIG

The proposed virtual inertia control (VIC) of DFIGs is developed from the maximum power point tracking (MPPT) control. Therefore, the dynamic model and MPPT control of DFIGs are briefly summarized at first.

In the synchronous dq reference frame, the flux vector, voltage vector, power and electrical torque can be expressed as

$$\psi_s = L_s I_s + L_m I_r$$
$$\psi_r = L_r I_r + L_m I_s$$
$$V_s = R_s I_s + \frac{d\psi_s}{dt} + j\omega_e \psi_s$$
$$V_r = R_r I_r + \frac{d\psi_r}{dt} + j(\omega_e - \omega_r)\psi_r \qquad (1)$$
$$P_s + jQ_s = -\frac{3}{2}V_s \hat{I}_s = -\frac{3}{2L_s}V_s(\hat{\psi}_s - L_m \hat{I}_r)$$
$$T_e = \frac{3}{2}p_D \text{Im}[\psi_s \hat{I}_s] = -\frac{3L_m}{2L_s}p_D \text{Im}[\psi_s \hat{I}_r]$$

where ω_e is the grid synchronous angular speed and ω_r is the rotor angular speed. V_s and V_r are the stator and rotor voltage vectors respectively. I_s and I_r are the stator and rotor current vectors respectively. ψ_s and ψ_r are the stator and rotor flux respectively. R_s and R_r are the stator and rotor resistances, and L_s and L_r are the stator and rotor inductances respectively. L_m is the mutual inductances and T_e is the electrical torque. P_s and Q_s are the stator output active and reactive power respectively, and p_D is the number of DFIG's pole pairs.

Using stator voltage oriented control, ignoring stator resistance and assuming constant stator flux , the electrical torque, total output active power and stator reactive power can be given by [7]

$$T_e = \frac{3pL_m}{2\omega_e L_s}V_s i_{rd}$$
$$P_e = \frac{3\omega_r L_m}{2\omega_e L_s}V_s i_{rd} \qquad (2)$$
$$Q_s = -\frac{3}{2L_s}V_s\left(\frac{V_s}{\omega_e} + L_m i_{rq}\right)$$

It can be seen from (2) that the decoupled control of the electromagnetic power/torque and the stator reactive power can be achieved by regulating the d- and q-axis rotor currents respectively.

Fig. 1 shows the overall vector control scheme of the RSC. The outer-loop control regulates the electromagnetic power and reactive power independently and generates the reference signals I_{rd}^* and I_{rq}^* for the inner-loop current regulation. The reference signal of the electromagnetic power P_{opt}^* is determined by the MPPT curve, which is shown in Fig.2. According to Fig.2, the reference value of the electromagnetic power can be expressed as

$$P_{opt}^* = \begin{cases} k_{opt}\omega_r^3 & (\omega_0 < \omega_r < \omega_l) \\ \dfrac{(P_{max} - k_{opt}\omega_l^3)}{(\omega_{max} - \omega_l)}(\omega_r - \omega_{max}) + P_{max} & (\omega_l < \omega_r < \omega_{max}) \\ P_{max} & (\omega_r > \omega_{max}) \end{cases} \qquad (3)$$

where k_{opt} is defined as the MPPT curve coefficient..
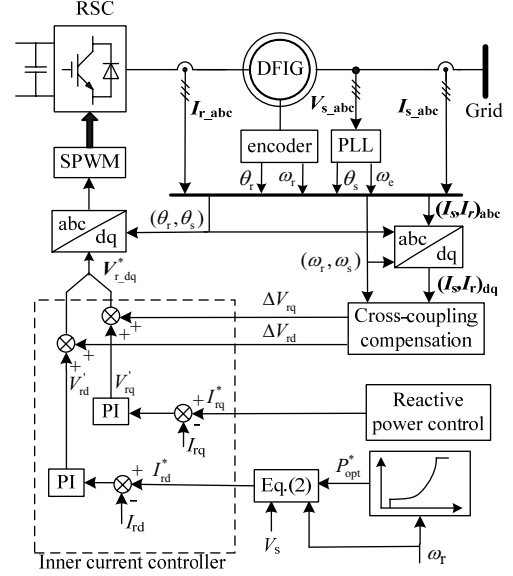

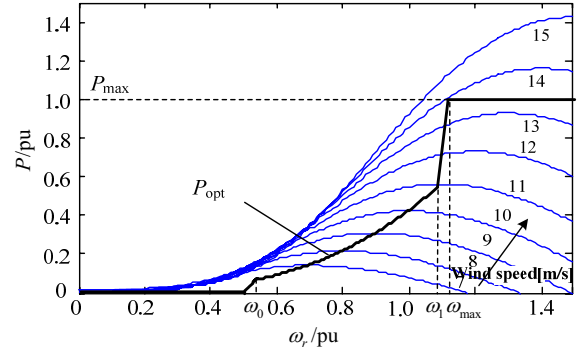Fig.1 Overall vector control scheme of the RSC

Fig.2 Maximum wind power point tracking curve

Under the MPPT control, the electromagnetic power can only be regulated according to the rotor speed, which is decoupled from the grid frequency. Therefore, the DFIG cannot contribute to system inertia in case of system power imbalance. In order to emulate the inertia response as synchronous generators using DFIGs, an improved control scheme by introducing the grid frequency deviation needs to be investigated.

3 Virtual inertia control of DFIGs

System inertia determines frequency change rate during a sudden power change. Synchronous generators and fixed speed wind turbines can automatically provide inertia support for an abrupt frequency change, while the variable speed wind turbines can not due to the decoupled operation between the

rotor speed and grid frequency. However, a variable speed wind turbine can emulate inertia even greater than its natural inertia by fast active power control.

3.1 Definition of DFIG virtual inertia

The kinetic energy stored in the rotating mass of a synchronous generator can be expressed as

$$E_k = \int (P_m - P_e)\, dt = \int J\omega_m d\omega_m = \frac{1}{2}J\omega_m^2 \qquad (4)$$

where ω_m is the rotor mechanical angular speed, J is the moment of inertia in the shaft.

Generally, the inertia constant of a synchronous generator is defined as the ratio of the total stored energy at the nominal speed ω_{mN} to the rated power P_N, i.e.

$$H = \frac{J\omega_{mN}^2}{2P_N} \qquad (5)$$

Hence, the inertia constant of the power system with DFIG-base wind farms can be expressed as

$$H_{tot} = \frac{\sum_{i=1}^{n}\left(\frac{1}{2p_i^2}J_i\omega_e^2\right) + \sum_{j=1}^{m}E_{k\_DFIG,j}}{S_{N\_tot}} \qquad (6)$$

where p_i and J_i are the number of pole pairs and moment of inertia for synchronous generator i respectively. S_{N_tot} is the nominal capacity of the grid, and $E_{k\_DFIG,j}$ is the kinetic energy stored in the rotating mass of DFIG-based wind turbine j. As $E_{k\_DFIG,j}$ can not be seen if MPPT control is used, thus there is

$$\sum_{j=1}^{m}E_{k\_DFIG,j} \approx 0 \qquad (7)$$

Therefore, operating a large number of DFIG-based wind turbines in place of conventional plants can significantly reduce the effective inertia of the system.

When the rotor speed of a DFIG changes from ω_{r0} to ω_{r1}, the kinetic energy available from the DFIG can be expressed by considering an equivalent synchronous generator whose rotor speed changes proportionally from ω_e to ω_{e1} as

$$\Delta E_{k\_DFIG} = \frac{1}{2}J_{DFIG}\left[(\omega_{r0}+\Delta\omega_r)^2 - \omega_{r0}^2\right]/p_D^2$$
$$= \frac{1}{2}J_{vir}\left[(\omega_e+\Delta\omega_e)^2 - \omega_e^2)\right]/p_D^2 \qquad (8)$$

where $\Delta\omega_e=\omega_{e1}-\omega_e$, and $\Delta\omega_r=\omega_{r1}-\omega_{r0}$. J_{DFIG} is natural inertia of the wind turbine and J_{vir} is DFIG's virtual inertia.

According to (8), the virtual inertia of the DFIG can be obtained as

$$J_{vir} = \frac{(2\omega_{r0}+\Delta\omega_r)\Delta\omega_r}{(2\omega_e+\Delta\omega_e)\Delta\omega_e}J_{DFIG}$$
$$\approx \frac{\Delta\omega_r}{\Delta\omega_e}\cdot\frac{\omega_{r0}}{\omega_e}J_{DFIG} = \lambda\frac{\omega_{r0}}{\omega_e}J_{DFIG} \qquad (9)$$

where $\lambda=\Delta\omega_r/\Delta\omega_e$, is defined as the virtual inertia coefficient.

Due to DFIG's asynchronous operation, the allowed DFIG speed variation is far wider than that of a typical synchronous generator. According to (5), the inertia constant of the DFIG can be defined as

$$H_{vir} = \frac{J_{vir}\omega_e^2}{2p_D^2 P_{N\_DFIG}} \qquad (10)$$

where P_{N_DFIG} is the rated capacity of the DFIG. Thus the total inertia time constant of the grid can be defined as

$$H_{tot} = \frac{\sum_{i=1}^{n}\left(\frac{1}{2p_i^2}J_i\omega_e^2\right) + \sum_{j=1}^{m}\left(\frac{1}{2p_{D,j}^2}J_{vir,j}\omega_e^2\right)}{S_{N\_tot}} \qquad (11)$$

It can be seen from (9) that the virtual inertia of the DFIG is determined not only by its nature inertia, but also by the pre-disturbance rotor speed ω_{r0} and the virtual inertia coefficient λ. Different from synchronous generators, whose rotor speeds are coupled directly to the system frequency, the speed variation of the DFIG may be much greater than the system frequency variation due to the asynchronous operation. Therefore, the virtual inertia of the DFIG can be several times of its natural inertia.

3.2 Virtual inertia control of DFIG

Based on the MPPT control, the VIC scheme proposed in this paper is designed to regulate the DFIG output active power reference according to the system frequency deviation to supply inertial contribution to the grid. The regulation of the active power reference is achieved by changing the MPPT curve coefficient k_{opt} to the VIC curve coefficient k_{VIC}, which is a function of system frequency deviation. From (3), it can be seen that different k_{VIC} will generate a series of power tracking curves, defined as VIC curves. The upper and lower limit of the VIC curves are defined as P_{VIC_max} and P_{VIC_min} (shown in Fig.3), respectively, to ensure that a steady operating point can be reached under any wind velocities.

3.2.1 Calculation of k_{VIC}

As shown in Fig.3, while the wind velocity is 9m/s, the DFIG operates at point A under the MPPT control initially. During an increase of system load, the grid frequency decreases. The DFIG is switched from the MPPT control to the VIC and the power tracking curve is shifted from the MPPT curve P_{opt} to the VIC curve (i.e., P_{VIC_max}) immediately. The operating point is thus moved from A to O and consequently the rotor decelerates and the kinetic energy stored in the rotating mass

is released to support the grid frequency. After the initial dynamic frequency response period, the DFIG operates at point B under the VIC.
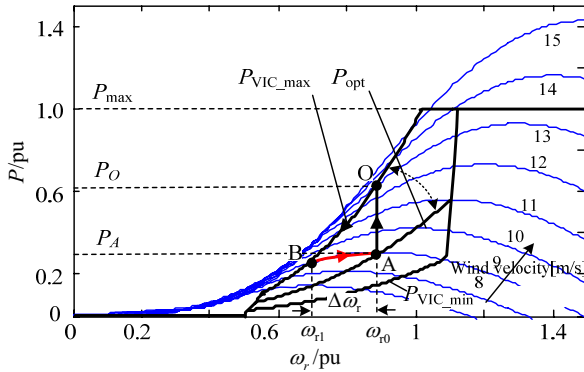

Fig.3 The scheme of the virtual inertia based power point tracking curve

Assuming that the wind velocity and the mechanical power of the DFIG remain constant, the relationship between the active power reference at point A and that at point B can be expressed as

$$k_{VIC}\omega_{r1}^3 \approx k_{opt}\omega_{r0}^3 \qquad (12)$$

where ω_{r1} can be expressed by frequency deviation

$$\omega_{r1} = \omega_{r0} + \Delta\omega_r = \omega_{r0} + \lambda\Delta\omega_e = \omega_{r0} + 2\pi\lambda\Delta f \qquad (13)$$

Substituting (13) into (12), the VIC curve coefficient k_{VIC} can be calculated as

$$k_{VIC} = \frac{\omega_{r0}^3}{\left(\omega_{r0} + 2\pi\lambda\Delta f\right)^3} k_{opt} \qquad (14)$$

Therefore, the VIC curve coefficient k_{VIC} is the function of the frequency deviation. The inertia control curves can be achieved by replacing k_{opt} with k_{VIC} in Eq. (3).

3.2.2 Principle of the VIC

The principle diagram of the VIC scheme is shown in Fig.4. A washed out function is used to eliminate the steady-state DC component of the frequency error.
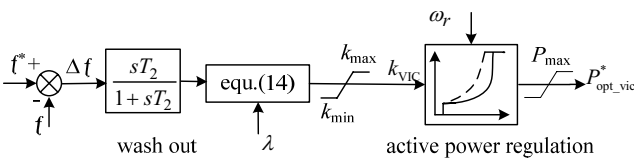

Fig.4 Principle diagram of the VIC

The dynamic response of the VIC can be divided into two stages: fast dynamic frequency support stage (A-O-B) and slow rotor speed recovery stage (B-A).

In the event of load increasing, the frequency will drop at the first stage. Thus k_{VIC} increases from the original value k_{opt} and reaches its upper limit rapidly. The corresponding power reference curve will then be shifted from P_{opt} to P_{vic_max}.

immediately. The DFIG operating point is shifted from A to O and its output power changes from P_A to P_O. Since the electrical power is greater than the mechanical power, the rotor decelerates and the operating point moves along the P_{vic_max} curve to B.

After the initial dynamic frequency response period, the frequency deviation will gradually reduce to zero with the power system primary and secondary frequency control. According to (14), the power reference curve will recover to MPPT curve, and the operating point is moved back from B to A. Thus the rotor speed of the DFIG recovers to the optimal value after the dynamic frequency support.

4 Simulation studies

Simulations have been carried out to illustrate the ability of the DFIG to emulate system inertia and to validate the proposed control scheme using Matlab/Simulink. A three-machine power grid shown in Fig.5 is used, which consists of two conventional power plants (G2, G3), three aggregated loads (L1, L2 and L3) and a DFIG-based wind farm rated at 1000 MW(500*2 MW). The G2 and G3 are rated at 3500 MW and 700 MW, respectively. The three loads L1, L2 and L3 are 1200 MW, 1500 MW and 600 MW respectively. The inertia constant of G2 and G3 are 5.2 s and 3.84 s respectively, and the natural inertia constant of the DFIG is 3 s. The G2 and G3 regulate frequency by their governors with 4% droop setting. Other parameters of the DFIG, G2 and G3 are given in appendix A. Comparative studies of network frequency responses with and without the proposed VIC following load sudden changes were carried out.
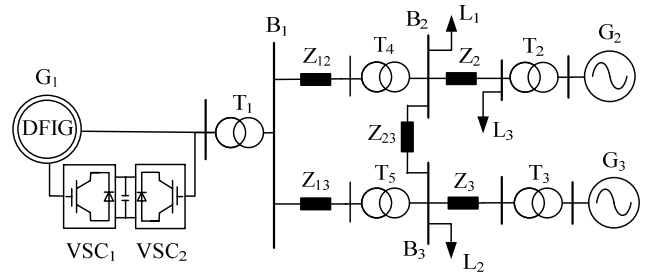

Fig.5 Structure of the simulation system

4.1 Sudden load increase

The wind velocity is 9 m/s and the DFIG is initially under the MPPT control. Load L1 is increased from 600 MW to 900 MW at 3s. Under the VIC scheme , the DFIG is switched from the MPPT control to the VIC when the frequency deviation is greater than 0.1Hz. Fig. 6 compares the frequency response with and without the VIC scheme. The virtual inertia of the DFIG is about 8 times of its natural inertia in this case (i.e. $\lambda=8$). It can be seen from Fig. 6 that the virtual inertia control improves the system performance significantly by increasing the minimum frequency point from 49.61 to 49.76Hz. It also considerably reduces the rate of the change of frequency. It can also be seen that the DFIG recovers to the MPPT control after 20s.
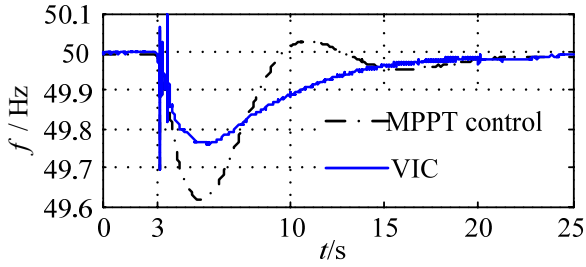
Fig.6 Comparison of the network frequency response during load L_1 sudden increasing 300MW
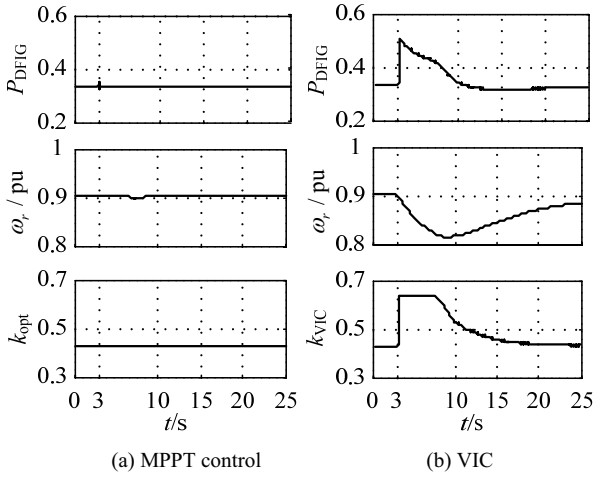

(a) MPPT control   (b) VIC

Fig. 7 The dynamic response of the DFIG during load L_1 sudden increasing 300MW

Figs. 7 (a) and (b) compare the dynamic responses of the active power, rotor speed and k_{VIC} with and without the VIC. It can be seen that for the conventional MPPT control the DFIG's active power and rotor speed remain constant, which indicates that the DFIG has no contribution to system frequency variation. In contrast, when VIC is implemented, the rotor speed decreases by 0.08 pu and the output active power increases by 0.18 pu. At the beginning of the frequency change, the VIC curve coefficient k_{VIC} increases rapidly and reaches its maximum value. When the frequency deviation reduces to zero, k_{VIC} goes back to k_{opt} gradually.

4.2 Sudden load decrease

Under similar conditions as previous case, simulation results of reduction of load L1 from 600 MW to 300 MW at 3s are shown in Figs. 8 and 9. Again, when the frequency deviation is greater than 0.1Hz, the DFIG is switched from the MPPT control to the VIC. Compared the frequency response with and without the VIC shown in Fig. 8, it can be seen that the VIC significantly improves system performance by decreasing the maximum frequency point from 50.39Hz to 50.28Hz. After 25 s the DFIG recovers to the MPPT control. In this case, $\lambda=6$.

Fig.9 (a) and (b) compare the dynamic responses of the active power, rotor speed and k_{VIC} with and without the VIC. It can be seen that with the conventional MPPT control the active

power and the rotor speed remain constant, whereas with the VIC the rotor speed increases by 0.05 pu and the output active power decreases by 0.08 pu. At the beginning of the frequency increase, the VIC curve coefficient k_{VIC} decreases rapidly. When the frequency deviation reduces to zero, k_{VIC} again goes back to k_{opt}.

Comparing the frequency responses shown in Fig.6 with $\lambda=8$ and that in Fig.8 with $\lambda=6$, it can be seen that larger λ can emulate more virtual inertia, and DFIGs with larger virtual inertia can provide better dynamic frequency support.
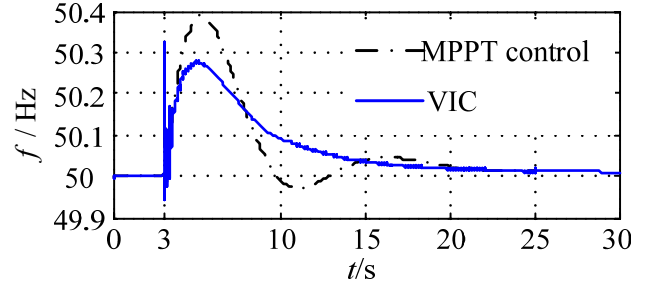

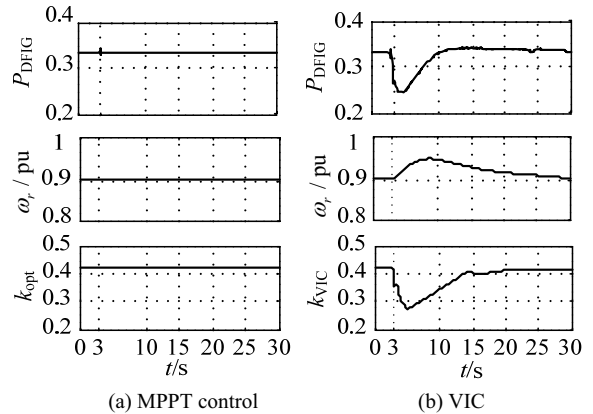Fig. 8 Comparison of the network frequency response during load L_1 sudden decreasing 300MW

(a) MPPT control   (b) VIC

Fig. 9 The dynamic response of the DFIG during load L_1 sudden decreasing 300MW

4.3 Comparison of the frequency responses of DFIG and SG

In order to illustrate the effect of VIC on system frequency response, three cases are considered, i.e., G1 being a synchronous generator with same capacity and inertia as the DFIG, G1 being the DFIG without inertia control, and G1 being the DFIG with the proposed inertia control. When load L1 is increased from 600 MW to 900 MW at 3 s, the system frequency responses for synchronous generator (line f_a), DFIG without inertia control (line f_b) and DFIG with the proposed inertia control (line f_c) are shown in Fig.10.

As shown in Fig.10, DFIG-based wind farm without inertia control results in the largest frequency drop due to the reduced effective total system inertia.. However, with the proposed VIC scheme, the DFIG can emulate inertia which is higher than that of the equivalent synchronous generator and

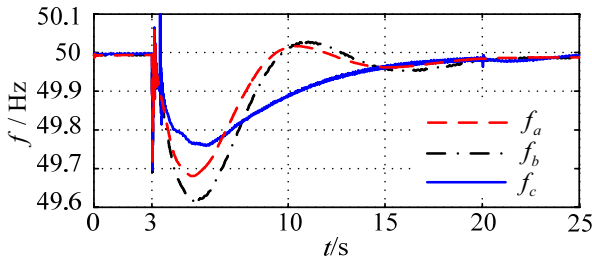consequently, it results in a significant improvement of system performance.

Fig. 10 Dynamic frequency response to a load increase

5 Conclusions

In the event of active power variation, system inertia determines the rate of frequency change. This paper investigates ways to make the "hidden inertia" of DFIGs available to the grid. The model and independent active and reactive power control strategy of DFIGs have been illustrated. The virtual inertia of the DFIG is defined and the virtual inertia control strategy is proposed. Fast dynamic frequency support is obtained by changing the active power reference of the RSC from the MPPT curve to the virtual inertia control curves. The rotor speed recovery to the optimal value is achieved. The proposed strategy is validated by simulation studies of a three-machine network. The results show that DFIG-based wind farms are able to emulate inertia by the proposed control and the virtual inertia can be larger than that of a equivalent synchronous generator due to DFIG's asynchronous operation.

Acknowledgements

References

[1] A. Mullane and M. O'Malley, "The inertial response of induction-machine-based wind turbines," *IEEE Trans. Power Syst.*, vol. 20, no. 3, pp. 1496–1503, Aug. 2005.

[2] J. Morren, S. de Haan, W. Kling, and J. Ferreira, "Wind turbines emulating inertia and supporting primary frequency control," *IEEE Trans.Power Syst.*, vol. 21, no. 1, pp. 433–434, Feb. 2006.

[3] G. Lalor, A. Mullane, and M. O'Malley, "Frequency control and wind turbine technologies," *IEEE Trans. Power Syst.*, vol. 20, no. 4, pp.1905–1913, Nov. 2005.

[4]. Juan Manuel Mauricio, Alejandro Marano, Antonio Gómez-Expósito, and José Luis Martínez Ramos. "Frequency regulation contribution through variable-speed wind energy conversion systems", *IEEE Trans. Power Syst.*, vol. 24, no. 1, pp. 173-180, Feb. 2009.

[5] Mustsfa Kayikci, Jovica V. Milanovic. "Dynamic contribution of DFIG-based wind plants to system frequency disturbances", *IEEE Trans. Power syst.*, vol. 24, no. 2, pp. 859-867, May 2009.

[6] Yi Wang, Xiaorong Zhu, Lie Xu, Heming Li. "Contribution of VSC-HVDC connected wind farms to grid frequency regulation and power damping", in *Proc. 2011 Indus. Electro. Conf.*, Phoenix, USA, 2010.

[7] Yi Wang, Lie Xu. "Coordinated control of DFIG and FSIG-based wind farms under unbalanced grid conditions", *IEEE Trans. Power Del.*, vol. 25, no. 1, pp. 367-377, 2010.

Appendix A

Tab.1 Parameters of the 2MW wind generator   pu

R_s	L_s	R_r	L_r	L_m	H	p
0.0108	0.102	0.01	0.11	3.362	3s	2

Tab.2 Parameters of the synchronous generator G2   pu

X_d	X_d'	X_d''	X_q	X_q''	R_s
2	0.35	0.252	2.19	0.243	0.0045
X_l	T_{d0}'	T_{d0}''	T_{q0}''	H	p
0.117	8	0.0681	0.9	5.2s	1

Tab.3 Parameters of the synchronous generator G3   pu

X_d	X_d'	X_d''	X_q	X_q'	X_q''	R_s
2.13	0.308	0.234	2.07	0.906	0.234	0.005
X_l	T_{d0}'	T_{d0}''	T_{q0}'	T_{q0}''	H	p
0.117	6.09	0.033	1.653	0.029	3.84s	1